Chapter 3

Iron(III) loaded novolac-based networks

for the removal of azo dyes from aqueous solutions

3.1 Introduction

With the rapid growth in the application of azo-dye colorants in many dyestuffs and allied industries, azo-dye pollution in water stream has become a serious environmental issue. Literature analysis in *Chapter-1* revealed that some of the azo dyes and their degradation products pose toxic, mutagenic and carcinogenic effects on human health and hazardous to aquatic organisms. Therefore, there is an urgent requirement to treat azo-dye laden effluents prior to discharge. Various physico-chemical methods have been used to remove azo dyes from colored effluents; adsorption as described in Chapter 1 has been recognized as the most popular treatment process because of its economics, design simplicity and efficiency in minimizing pollutants, easy recovery and reusability of adsorbents. It is also discussed in *Chapter-1* that the polymeric sorbents exert exclusive attributes in removing dye pollutants from wastewaters. Polymer/inorganic hybrid materials represent an emerging group of adsorbents that have attracted interest to remove trace pollutants from waters[3.1-3.3]. Their unique properties arise from the combination of both polymer and inorganic characteristics. They exhibit higher adsorption capacity than polymer because of their hybrid nature comprising two phases both of which contribute to adsorption of pollutants. Efforts are being undertaken in *Chapter-2* to explore utilization of novolac type phenolic resin in the preparation of network adsorbents (**2.3**, **2.4**) for azo dye removal. Adequate

functionality including porosity in these network structures can allow interaction with metal ions constituting new type of polymer/inorganic hybrid materials. As an extension in this research direction, a compilation of our published paper[3.4] (included in the Appendix) focusing on the preparation of iron (III) loaded novolac-based networks is presented in this chapter along with key findings on azo dye adsorptive removal performance. To the best of our knowledge, no literature is available on azo dye removal by such hybrid materials.

3.2 Objective

This chapter aims to describe the preparation of iron (III) loaded novolac-based networks **3.1** and **3.2** (Figure 3.1) as hybrid adsorbent materials showing high performance on azo dye removal from aqueous solution.

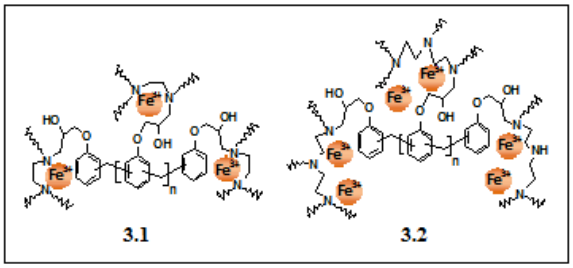

Figure 3.1. Iron(III) loaded novolac-based networks **3.1** and **3.2**

3.3 Experimental Section

3.3.1 Materials and Measurements

Chemicals were purchased and used without purification. FTIR spectra were recorded on Perkin Elmer spectrophotometer using KBr discs. X-ray diffraction pattern was recorded using X-ray diffractometer (*Rigaku*) with Cu K_α radiation (λ = 1.5418Å) and scanning angle 2θ between 20^o and 80^o. Thermogravimetric analysis (TGA) was conducted using Perkin Elmer STA 6000 instrument under nitrogen atmosphere. UV-vis spectra were recorded on ShimadzuUV-1800 spectrophotometer. A pH meter (Tosniwall, CL 46) was employed for the pH measurements.

3.3.2 Synthesis of iron(III) loaded novolac-based network adsorbents

Hybrid adsorbents **3.1** and **3.2** were prepared using $Fe(NO_3)_3$ and novolac-based precursor networks **2.3** and **2.4**. The preparation method of precursors (2.3, **2.4**) was described in Chapter 2. In a typical preparation, network and iron(III) nitrate nonahydrate [$Fe(NO_3)_3$.9H2O] were first mixed in the ratio (1:10 , w/w) in deionised water and left for adsorption for 24h. The network was then filtered, and impregnated with deionized water for another 24h. The solid separated by filtration, washed thoroughly with deionized water and dried for 12h at 50-60 ^{0}C to yield Fe(III) loaded network. The filtrates and washings were combined. The amount of Fe(III) loaded onto the network was evaluated by measuring the concentration of Fe^{3+} remaining in combined

solution using UV-vis spectrophotometric method by measuring maximum absorbance of ferric thiocyanate color complex, located at λ = 480 nm. Graphical plot of absorbance (y axis) against Fe^{3+} (aq) concentration was used to find the concentration of Fe^{3+} in aqueous solution after adsorption. Iron content in **3.1** and **3.2** were estimated to be 38 mg g^{-1} and 85 mg g^{-1} respectively.

3.3.3 Adsorption experiments

The batch adsorption experiments were conducted by adding pre-weighed amount of sorbents to the aqueous solution of azo dye at pH 7.20 and shaken at room temperature. The pH was adjusted to a given value with dilute NaOH or HCl solutions. The solutions were periodically separated from the adsorbents, and the residual concentrations of azo dyes were estimated by UV-vis spectrophotometer at λ_{max} = 484 nm. The amount of dye adsorbed (mg/g) at equilibrium was calculated by using the formula:

$$q_e = \frac{(C_0 - C_e)V}{W}$$

where C_0 and Ce are the initial and equilibrium dye concentrations (mg/L) respectively. V is the volume of solution (L) and W is the weight of the sample (g).

Freundlich isotherm model[3.5-3.7] was employed to assess the adsorption equilibrium.

The logarithmic form of the Freundlich equation is represented by the following equation:

$$\ln q_e = \ln K_f + 1/n \ln C_e$$

where K_f and n are Freundlich constants related to the adsorption capacity and adsorption intensity, respectively. K_f and 1/n were obtained from the linear plot of $\ln q_e$ vs. $\ln C_e$.

3.3.4 Desorption and reusability study

Azo-dye loaded adsorbents were kept in deionised water and the pH of the medium was adjusted to 12.0 by adding dilute NaOH solution. The mixtures were shaken at 25^{o}C for a period of 24h to desorb azo dyes (MO/OG). Then adsorbents were separated and analyzed for dye concentration in desorbent water using UV-vis spectrophotometer. Desorption amount was calculated using the following equation.

$$\text{Desorption (\%)} = \frac{(C_{des} \times V_{des})}{(C_0 - C_e)\, V_{ads}} \times 100$$

Where V_{des} = volume of desorbent used,

C_{des} = final concentration of azo dye in solution after desorption

Thereafter, the regeneration process of adsorbents was performed by putting them in fresh deionised water. The pH was adjusted to neutral with dilute HCl. The resulting regenerated sorbents were filtered, dried and reused in the next cycle. The adsorption/desorption process was repeated three times.

3.4 Results and discussion

3.4.1 Synthesis and characterization

Novolac-based network precursors **2.3** and **2.4** deserve particular attention in loading metal ions especially ferric minerals, due to the nonhydrolyzable polyfunctionality in combination with the feature of novolac structural support providing mechanical, chemical, and thermal strength. The ligating groups (amino, hydroxyl) in their porous structures could allow incorporation of Fe(III). This might avoid dissolution of Fe(III) in the medium during waste treatment applications. In addition, ferric minerals were found to have use in separation process[8] because of their ready availability and chemical stability. Also they are inexpensive and harmless. Thus incorporation of such inorganics tends to be an innovative strategy for obtaining polymer/inorganic hybrid adsorbent materials. Scheme 3.1 illustrates the loading of Fe(III) ions in the networks to yield **3.1** and **3.2**.

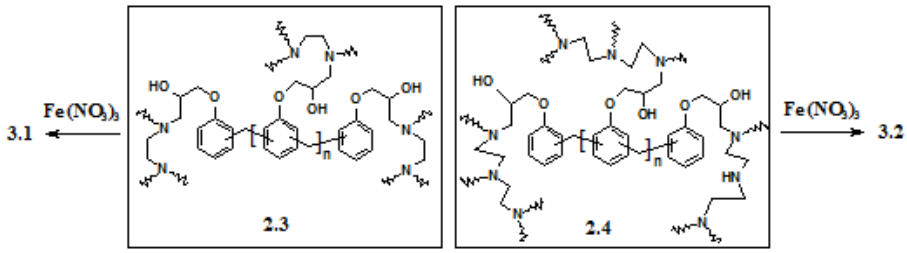

Scheme 3.1. Preparative scheme for iron(III) loaded novolac-based networks **3.1** and **3.2**

The resulting hybrids were characterized by FTIR, XRD and TGA analyses. FTIR spectra of **3.1** and **3.2** (Figures 3.2 and 3.3) show the broad band

located in the region 3000 – 3500 cm^{-1}, assignable to the O-H and N-H stretching frequencies.

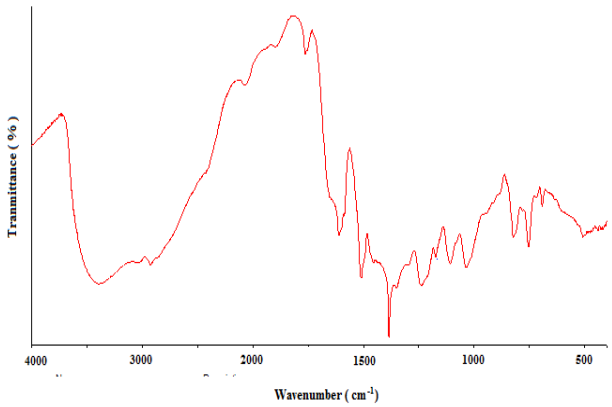

Figure 3.2 FTIR spectrum of **3.1**

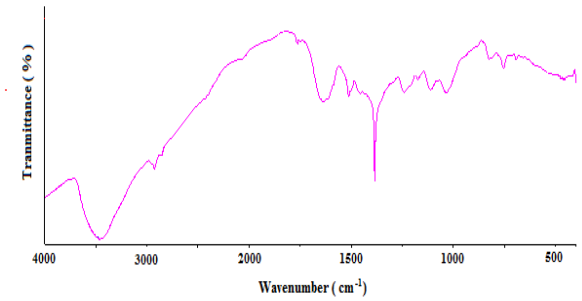

Figure 3.3 FTIR spectrum of **3.2**

Compared to **2.3** and **2.4** (data given in *Chapter-2*), this band was found to be further broadened and shifted to longer wavenumbers ($\Delta\nu$ = 25-30 cm^{-1}) indicating the involvement of ferric ions in coordination with amino and hydroxyl moieties in association with the coordinated water molecules. Furthermore, there were shifts to longer wavenumbers ($\Delta\nu$ = 6-27 cm^{-1}) of O–

H bending vibrations appearing at 1610 cm^{-1} and 1627 cm^{-1} when iron loaded onto the networks. The shifting of these peaks to longer values underlines the presence of coordinated OH groups in the networks. The absorption band near 1382 cm^{-1} appeared due to the vibrations of nitrate ions[3.9,3.10], which confirms the incorporation of ferric nitrate in the networks.

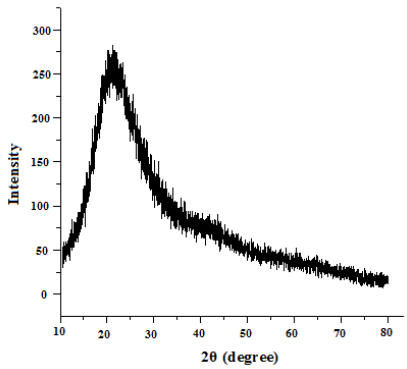

Figure 3.4 The XRD pattern of **3.2**

Figure 3.4 shows the XRD pattern of **3.2**. The pattern showing broad peak centred at 2θ = ~ 21.22º and very low intensity peak centred at 2θ = ~ 40.75º was characteristic for amorphous material. The appearance of no sharp peaks further indicates the amorphous structure of Fe^{3+} salt loaded within the polymer matrix. This could be advantageous since amorphous compounds are known to be especially effective in achieving adsorption compared to crystalline forms[11].

Thermal properties of **3.1** and **3.2** were examined by TGA. The results are summarized in Table 3.1. Thermograms for **3.1** and **3.2** exhibited thermal stability of up to 204 ^{o}C and 208 ^{o}C, respectively with low rate of weight loss (15%) which might be due to the release of trapped water molecules. All showed a four-step dramatic weight loss of 40 – 50% at the temperature range 200 – 450^{o}C, which was ascribed to the decomposition of polymeric matrix along with Fe(III) nitrates. Thermal degradation curves further showed a weight loss with slower slope upto 500^{o}C. However, compared to the neat novolac-based networks (**2.3**, **2.4**), Fe(III) loading imparts lowering of onset temperature of decomposition of the resulting hybrids (**3.1**, **3.2**).

Table 3.1 Thermal properties (TGA) of **3.1** and **3.2**

Hybrid	T_d^{15}(^{o}C)	Stage	Temp. range (^{o}C)	Weight loss %
3.1	204	1	204-260	15.05
		2	260-308	8.85
		3	308-430	17.28
		4	430-500	7.84
3.2	208	1	208-250	15.98
		2	250-305	12.61
		3	305-440	21.03
		4	440-500	4.21

TGA was performed at a heating rate of 10^{o}C/min under nitrogen flow; T_d^{15} = Temperature at which 15% weight loss occurred.

3.4.2 Azo dye adsorption studies

The popular azo dyes like methyl orange (MO) and orange-G (OG) whose characteristics and chemical structures are illustrated in *Chapter-2* were employed as representative dyes in the evaluation of adsorption abilities of **3.1** and **3.2**. Azo dye adsorption onto hybrid materials was studied as a function of contact time at pH 7.20. Adsorbents exhibit significant dye removal behaviour for MO and OG as estimated from the decrease in maximum absorbance at 484 nm. As shown in Figure 3.5, the rapid adsorption at the initial stage was occurred and reached a nearly equilibrium within 48 h. This could probably be attributed to the abundance of unoccupied adsorption sites. The dye adsorption gradually slowed down with time which is probably associated with the slow diffusion of the dye molecules into the sorbents porous structures. The rapid adsorption at the initial stage demonstrates the suitability of the sorbents in reducing reactor volumes and times.

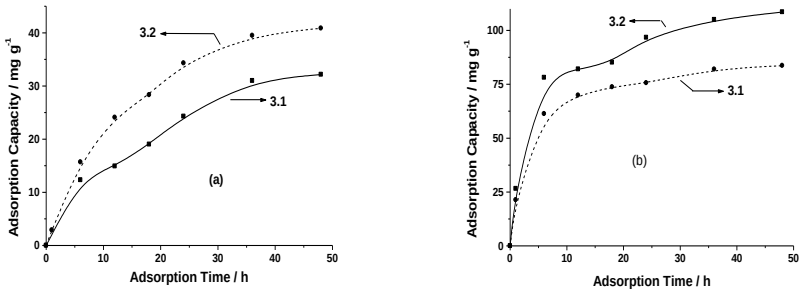

Figure 3.5 The effect of adsorption time on azo-dye adsorption of **3.1** and **3.2** at pH = 7.20 (a) MO adsorption (C_0 = 50 mg L^{-1}; 1.52 x 10^{-4}M); (b) OG adsorption (C_0 = 150 mg L^{-1};3.31 x 10^{-4}M).

Figure 3.6 displays the effect of Fe(III) loading on the adsorptive removal of MO and OG. **3.2** has higher Dye adsorption was found to be quite higher for **3.2** as compared to **3.1** due to higher loading of Fe(III). The results of azo-dye removal by designed networks (**2.3**, **2.4**) were reported in *Chapter-2*. However, under comparable conditions hybrids (**3.1**, **3.2**) achieved higher adsorption capacities than networks (**2.3** , **2.4**) which was attributed to the role of Fe(III) being immobilized onto the networks. In addition, higher uptake was for OG by hybrid sorbents indicating more favorable interaction.

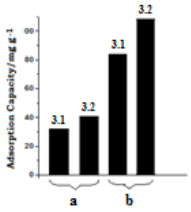

Figure 3.6 Azo dye adsorption capacity of **3.1** and **3.2** (pH = 7.20; t = 48h; T= 298 K); (a) MO adsorption (C_0 = 50 mg L^{-1}; 1.52 x 10^{-4}M); (b) OG adsorption (C_0 = 150 mg L^{-1}; 3.31 x 10^{-4}M)

The visual changes in color of the azo dye solutions from red to very light yellow during the same process were recorded in Figure 3.7. This result demonstrates the effective adsorptive response of sorbents in color removal.

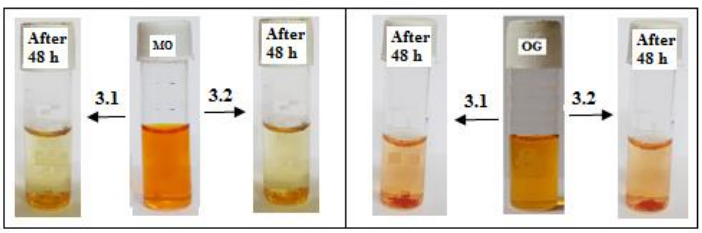

Figure 3.7 Color changes of MO and OG solutions before and 48 h after adsorption onto **3.1** and **3.2** at pH = 7.20

Meanwhile, the adsorbents **3.1** and **3.2** turned to deep red and orange after adsorbing MO and OG, respectively (Figure 3.8). This accounted for a visual indication of MO/OG loaded sorbent surfaces.

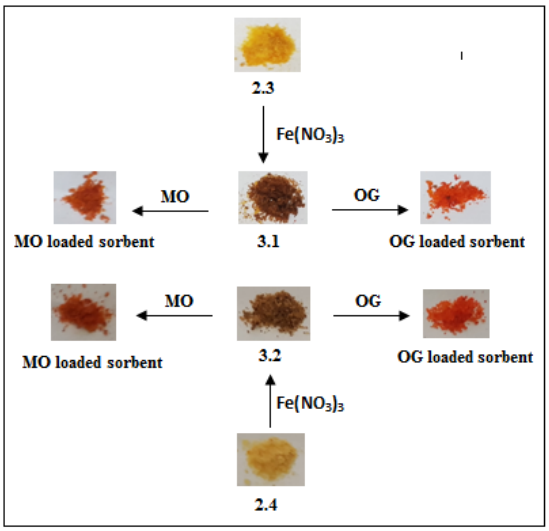

Figure 3.8 Photographs of sorbents on adsorption of MO and OG after 48h

Freundlich model was used to fit the equilibrium adsorption isotherm data. The model parameters (n, K_f) along with the correlation coefficients (R^2) were obtained from the graphical plots of ln q_e against ln C_e as presented in Figures 3.9 and 3.10. The values of these parameters were listed in Table 3.2. The K_f values revealed the good adsorption capacity of both **3.1** and **3.2**. The value of n in the range 1-10 indicated thermodynamically favorable adsorption. The values of R^2 reflected adequate description of dye adsorption by Freundlich isothermal model. Therefore, iron loading in the networks provides new kind of materials applicable in the manipulation of azo dye adsorption capacities.

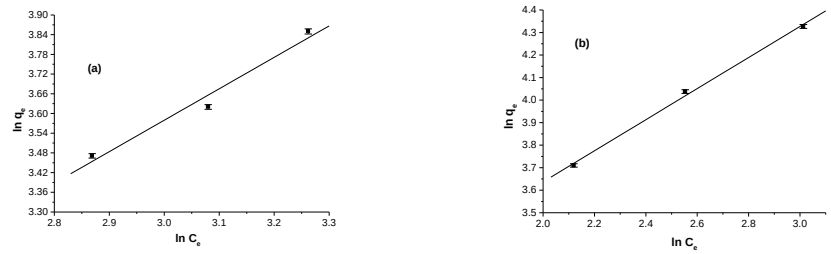

Figure 3.9 Freundlich isotherms for the adsorption of MO onto (a) **3.1** and (b) **3.2** [pH 7.20, temperature: 25ºC]

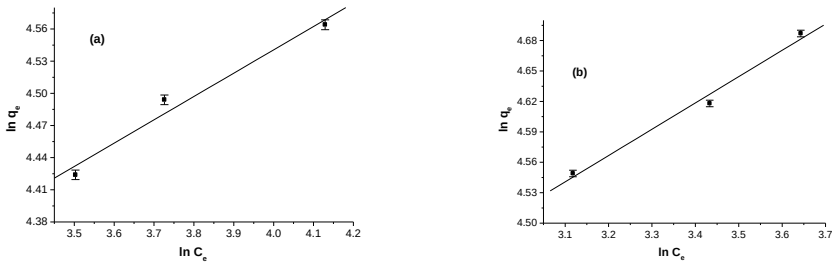

Figure 3.10 Freundlich isotherms for the adsorption of OG onto (a) **3.1** and (b) **3.2** [pH 7.20, temperature: 25^{o}C]

Table 3.2 Freundlich fitting parameters in MO and OG adsorption isotherms for the studied samples at pH 7.20

Fe(III) loaded polymer network	Azodye	Freundlich Constants		
		K_f	n	R^2
3.1	MO	2.027	1.044	0.9729
	OG	39.251	4.594	0.9731
3.2	MO	9.550	1.448	0.9971
	OG	41.952	3.855	0.9868

The qualitative information on the chemical interactions was obtained from the FTIR spectral analysis of the dye-adsorbed networks (dry). The broad

absorption band in the region 3200 – 3500 cm^{-1} (O-H and N-H stretching) experienced better resolution when dye adsorbed. In addition, the stretching vibrations of azo-dye SO_3^- groups shifted to lower wavenumber ($\Delta\nu$ = 2-9 cm^{-1}) appearing at 1171 and 1033 cm^{-1} with reduced intensity when loaded onto the sorbents. This is ascribed to the interaction of sorbents with azo dyes through SO_3^- groups. The decrease in intensity of the NO_3^- peak (1382 cm^{-1}) also occurred, which indicated ion exchange sorption of anionic azo dye molecules.

3.4.3 Desorption and reusability study

To further explore the reusability, the adsorption-desorption cycle was repeated upon pH adjustment with dilute HCl or NaOH solutions. As presented in Figure 3.11, the desorptions are visually followed by gradual disappearance of sorbents colors, and the color development in aqueous solutions. More than 90% desorption was found to happen during 24h in the alkaline condition ((pH ≈ 12.0). UV-vis spectral investigation quantified the desorbed amount of azo dyes (MO/OG). After desorption the sorbents were regenerated by pH adjustment to 7.0 and reused for a number of cycles for its adsorption efficacy. However, adsorption efficiency remained comparable with increasing cycle number. After three consecutive cycles, the azo dye adsorption efficiency is still above 80%. This is quite important not only in the effective regeneration and reuse of the sorbents, but also the reuse of

recovered azo dyes during the dyeing process impacting associated environmental issue.

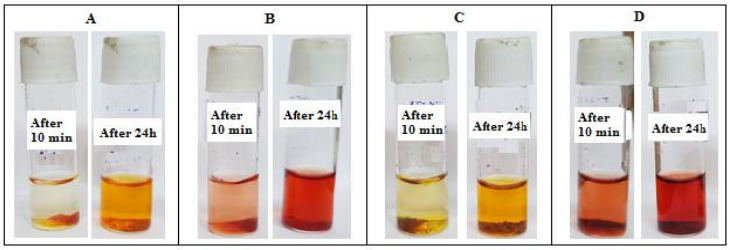

Figure 3.11 Desorption of MO and OG from dye loaded networks in water at pH = 12.0 (A) MO loaded **3.1** (B) OG loaded **3.1**(C) MO loaded **3.2** and (D) OG loaded **3.2**.

3.4.4 Adsorption-Desorption Mechanism

On the basis of author's reports[3.12-3.14] given in *Chapter-2* and experimental observations, the proposed mechanism for dye adsorption and desorption is outlined in Figure 3.12. In this context, structures of MO and OG and iron species loaded onto the network having a variety of interacting motifs (amino, hydroxy and ether functionalities) must be taken into account. Iron species might create more active sites synergic with functional adsorptive motifs of networks to cater more azo dye pollutants on the surface. The involvement of physical forces, such as metal ion coordination as well as hydrogen bonding interactions involving functional groups of dye molecules (Fe^{3+}---$^{-}O_3S$–Dye, and Network–O-H---$^{-}O_3S$– etc) might account for higher adsorption capacity (Figures 3.6, 3.7). It is worth to note the occurrence of desorption of azo dyes

from sorbents in the very basic condition (pH ≈ 12.0). This likely is related to the change of Fe^{3+} to $Fe(OH)_3$ and other complex hydroxides embedded in the network, which make the materials redundant favoring desorption. In addition, desorption might be related to the high enough concentration of hydroxyl ions (OH^-) competing with the anionic dye molecules (Dye-SO_3^-) for adsorption sites.

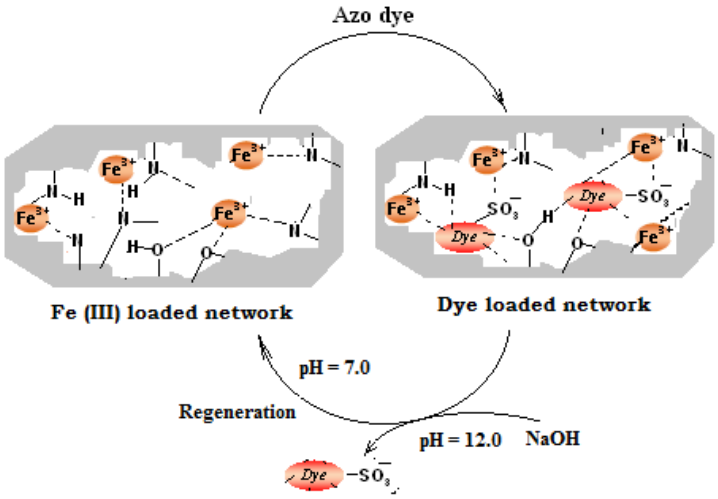

Figure 3.12 A proposed mechanism of adsorption-desorption of azo dye pollutants onto the hybrid sorbents

3.4.5 Importance of the work

Combining features of novolac-based networks and inorganic characteristics of iron salt, hybrid adsorbents show enhanced dye adsorption performance. Because of the simplicity in preparation, high adsorption capacity and reusability, the hybrid sorbents should have high potential for applications in

remediation technology and environmental sciences aiming to the treatment of azo dye-laden wastewaters and analytical chemistry.

3.5 Conclusion

This chapter gives a new way to prepare novolac-based network-Fe(III) hybrid adsorbents. The resulting hybrids were characterized by FTIR, XRD and thermal (TGA) analyses. Iron(III) loading onto the novolac-based networks imposes enhanced removal of MO and OG from aqueous solution. Adsorbent **3.2** with more iron(III) content shows high adsorptive removal of azo dye pollutants. Equilibrium adsorption phenomenon was expressed using Freundlich isotherm. The result indicates that adsorption is a typical physical process ($n > 1$). The feasible mechanism toward azo dye removal was proposed. Quite effective adsorption-desorption-regeneration-reuse cycle under pH adjustment offers great economic potential for remediation of azo-dye containing wastewaters.

3.6 Further scope of work

The author recommends further research:

i) Further research to investigate the adsorption capacities of such hybrid adsorbing materials toward a variety of azo dye colorants is required.

ii) In view of advanced oxidation processes (AOPs) the prepared hybrid adsorptive systems might be utilized as heterogeneous Fenton like decoloration of captured azo dye pollutants. Network immobilized Fe(III) in presence of H_2O_2 is believed to provide such oxidative systems. Further investigation in this direction is needed.

iii) Presented hybrid adsorptive systems recommend further investigation in removing azo dye colorants from real industry wastewater samples.